V-ATPase inhibition decreases mutant androgen receptor activity in castrate-resistant prostate cancer

Bradleigh Whitton[1,2], Haruko Okamoto[3,4], Matthew Rose-Zerilli[1,2], Graham Packham[1,2], Simon J. Crabb[1,2*]

[1]Cancer Sciences Unit, Southampton General Hospital, Tremona Road, Southampton, SO16 6YD, UK
[2]Cancer Research UK Centre, University of Southampton, Southampton General Hospital, Tremona Road, Southampton, SO16 6YD, UK
[3]School of Biological Sciences, University of Southampton, Highfield, Southampton, UK
[4]School of Life Sciences, University of Sussex, Falmer, Brighton, BN1 9QG, UK

Running title: V-ATPase inhibition and AR activity in prostate cancer

Key words: androgen receptor, prostate cancer, V-ATPase, castrate resistant

Corresponding author*: Dr Simon Crabb, Cancer Sciences Unit, Southampton General Hospital, Tremona Road, Southampton, SO16 6YD, UK.
S.J.Crabb@southampton.ac.uk

Conflict of interest statement: SJC has received fees for advisory work from Roche, Janssen Cilag, MSD, Pfizer and Bayer and research support from AstraZeneca, Astex Pharmaceuticals and Clovis Oncology. The other authors declare no potential conflict of interest.

Abstract

Prostate cancer (PC) is critically dependent on androgen receptor (AR) signaling. Despite initial responsiveness to androgen deprivation, most patients with advanced PC subsequently progress to a clinically aggressive castrate-resistant (CRPC) phenotype, typically associated with expression of splice-variant or mutant AR forms. Although current evidence suggests that the vacuolar-ATPase (V-ATPase), a multi-protein complex that catalyzes proton transport across intracellular and plasma membranes, influences wild-type AR function, the effect of V-ATPase inhibition on variant AR function is unknown.

Inhibition of V-ATPase reduced AR function in wild-type and mutant AR luciferase reporter models. In hormone-sensitive PC cell lines (LNCaP, DuCaP) and mutant AR CRPC cell lines (22Rv1, LNCaP-F877L/T878A), V-ATPase inhibition using bafilomycin-A1 and concanamycin-A reduced AR expression, and expression of AR target genes, at mRNA and protein levels. Furthermore, combining chemical V-ATPase inhibition with the AR antagonist enzalutamide resulted in a greater reduction in AR downstream target expression than enzalutamide alone in LNCaP cells. To investigate the role of individual subunit isoforms, siRNA and CRISPR-Cas9 were used to target the V_1C1 subunit in 22Rv1 cells. Whereas transfection with ATP6V1C1-targeted siRNA significantly reduced AR protein levels and function, CRISPR-Cas9-mediated V_1C1 knockout showed no substantial change in AR expression, but a compensatory increase in protein levels of the alternate V_1C2 isoform.

Overall, these results indicate that V-ATPase dysregulation is directly linked to both hormone responsive and CRPC via impact on AR function. In particular, V-ATPase inhibition can reduce AR signaling regardless of mutant AR expression.

Introduction

Prostate cancer (PC) was diagnosed in 1.28 million men, and caused 359,000 deaths, in 2018 (1). Initially, prostate cancer cell growth is dependent on androgen receptor (AR) activation. Advanced disease is therefore treated with permanent androgen deprivation therapy (ADT), to limit cancer cell growth (2). However, subsequent progression from a hormone sensitive (HSPC) to a more aggressive castrate resistant (CRPC) phenotype is almost inevitable. Metastatic CRPC treatment options include hormonal therapy (abiraterone, enzalutamide), chemotherapy and radium-223. However, CRPC outcomes remain poor with a median survival of around 2 years (2).

CRPC prognosis is partly attributed to persistent AR signaling through adaptive alterations to the AR itself. AR alterations are relatively rare at PC diagnosis but become more prevalent through ADT/hormonal therapy exposure and represent a key mechanism for transition to CRPC (3). Gain-of-function point mutations, particularly in the ligand-binding domain (LBD), may provide growth advantage despite a castrate state. For example, the F877L AR mutation converts some second-generation antiandrogens (e.g., enzalutamide, apalutamide), to agonist function (4). The F877L mutation has been observed in enzalutamide resistant PC xenograft models (5) and detected in plasma DNA of CRPC patients previously treated with apalutamide (4). T878A is a further well characterized AR point mutation (6) that converts AR antagonists (e.g., flutamide) to agonists (7), and broadens AR ligand binding-specificity, for example to progesterone (8). This mutation was found in abiraterone treated CRPC patients producing a progesterone-activated abiraterone resistant state (9).

AR splice variants (AR-V) are truncated AR forms, resulting in ligand independent constitutive activation, through loss of a LBD portion and represent a further CRPC transition mechanism (10). The most common, AR-V7, is associated with enzalutamide and abiraterone resistance (11), and reduced survival (12). AR-V7 expression is heterogeneous, and may heterodimerise with full-length AR, or form homodimers, to bind AR response elements (AREs) to facilitate a protumorigenic transcriptome (13). AR-V7 mRNA expression has

been found 20-times higher in CRPC patients than in HSPC patients (14), and protein levels of AR-V7 have been shown to increase on development of CRPC (15).

Vacuolar-ATPase (V-ATPase) is a multi-protein complex that catalyzes ATP-dependent proton transport across intracellular and plasma membranes. The resulting acidification of organelle lumens or extracellular space influences a diverse range of cellular processes, many of which are dysregulated in cancers (16). V-ATPase is composed of two domains, the cytosolic V_1 domain and the integral membrane complex, V_O. V_1, which is responsible for ATP hydrolysis, is composed of 8 subunits (A-H), whereas V_O, responsible for proton translocation across the endo-membrane, is composed of 5 (a, c, c'', d, e) (17). The V_1 domain is tethered to the V_O domain via the V_1 subunit V_1C, which is important in regulating enzyme disassembly (18). In addition to its proton pump function, V-ATPase is now understood to have a central role in sensing environmental signals, including pH (19), and is required for amino acid mediated mTORC1 signaling (20).

Limited data indicate a potential role of V-ATPase in PC and, in particular, on AR modulation. V-ATPase expression correlates to invasive and metastatic potential of PC cells as evidenced by; (i) its expression in the plasma membrane (PM), (ii) V-ATPase dependent activation of proteases (e.g., MMP-2, -9, -14), and (iii) increased cell motility (21). Evidence suggests that the V_Oa3 isoform (and potentially V_Oa1, V_Oa2 and V_Oa4) plus the V-ATPase accessary subunit Ac45, are key in targeting V-ATPase to the PM in PC cells (22). Additionally, individual subunit isoform knockdown resulted in reduced proton flux and V-ATPase function (22), and chemical inhibition caused alkalization of endo-lysosomal compartments (23). V-ATPase modulatory proteins such as LASS2/TMSG1 and PEDF can affect tumor cell growth and invasion via regulation of V-ATPase activity (24,25). Chemical inhibition of V-ATPase in HSPC (LNCaP) and CRPC (C4-2B) cell lines reduced in vitro invasion of both (26). Additionally, V-ATPase co-localised with PSA and V-ATPase inhibition resulted in a PSA relocalization to lysosome-like intracellular vesicles (26). Furthermore, V-ATPase inhibition in LNCaP and LAPC4 cells depleted both AR protein and mRNA (23).

These data support a potential link between AR and V-ATPase function in PC. We provide data to explore this interaction, including for altered AR forms relevant for clinical transition to CRPC.

Materials and Methods

Reagents and cell lines

HEK-293 and LNCaP/DuCaP/22Rv1 cells were maintained in Dulbecco's Modified Eagle's Medium (Sigma) and Roswell Park Memorial Institute (RPMI) medium (Sigma) respectively, supplemented with 10% fetal bovine serum (FBS) with 4 mM or 2 mM L-glutamine respectively and 1 mM pyruvate. Where indicated, media was changed at 24 hours to phenol-red free RPMI-1640 (Life Technologies) supplemented with 10% charcoal stripped FBS (CSS-RPMI) (Life Technologies). LNCaP F877L/T878A and LNCaP control empty plasmid cells were a gift from Novartis (5). All cell lines were regularly mycoplasma tested and passaged between 15-30 times for all experiments. Enzalutamide was purchased from Selleckchem, bafilomycin-A1 (baf-A1) from Melford and dihydro-testosterone (DHT) and concanamycin-A from Sigma Aldrich. Compounds were dissolved in dimethyl sulfoxide (DMSO). Cell viability was assessed using the MTS assay (Sigma) as per the manufacturer's instructions.

Dual luciferase reporter assay

Briefly (as previously described ((27)), HEK-293 cells were transfected with the androgen response element (ARE) reporter plasmid p$(ARE)_3$Luc, wild-type of mutant/variant AR expression plasmids (pEAR-WT/pEAR-V7/pEAR-Q641X/pEAR-F877L) and pRL-CMV (control *Renilla* luciferase expression plasmid) using Fugene HD transfection reagent (Promega). The AR-V7 and AR-Q641X expression plasmids were a gift Jocelyn Ceraline, University of Strasbourg (28). The dual luciferase reporter assay (Promega) was performed using the Varioskan™ Flash Multimode Reader (ThermoScientific). Results show firefly luciferase activity normalized to *Renilla* luciferase activity as a transfection efficiency control.

RT-qPCR

Total mRNA was extracted using the ReliaPrep RNA Cell Miniprep System

(Promega) following manufacturer's instructions and quantified using a NanoDrop (ThermoScientific). For cDNA synthesis, M-MLV Reverse Transcriptase (Promega) followed manufacturer's instructions. For qRT-PCR, TaqMan® Universal PCR Master Mix, No AmpErase® UNG (ThermoFisher Scientific) utilized commercially available TaqMan® Gene Expression Assays probes for *KLK3* (PSA), *TMPRSS2* and the reference gene *GAPDH*. The 7500 Real-Time PCR thermal cycler machine (Applied BioSystems) was used for the RT-qPCR reaction via thermo-cycling and detection of subsequent fluorescence. The Real-Time qPCR software v2.0.6 (Applied BioSystems) then calculated Ct values and the comparative $2^{-\Delta\Delta C(T)}$ method as described (27) to calculate fold changes in gene expression.

Western blot analysis

Whole cell lysates were collected in 1x RIPA buffer and fragmented using sonication. Proteins were quantified using the Bradford assay (Promega), separated using SDS-PAGE, transferred to a nitrocellulose membrane (Amersham Protran 0.45 NC, GE healthcare) and blocked in PBS-T with 5% milk solution. Membranes were probed with primary antibodies to AR, PSA (Cell Signaling), ATP6V1C2 (Santa-Cruz), ATP6V1C1, ATP6V1A (Invitrogen) and β-Actin (Sigma) followed by horse radish peroxidase conjugated anti-mouse or anti-rabbit IgG secondary antibodies (Sigma). Detection was with enhanced chemiluminescent reagents (ThermoFisher). Immunoblot signals were quantified using ImageJ (http://imagej.nih.gov/ij/) and protein expression was normalized to β-Actin.

siRNA transfection

Experimental (ON-TARGETplus Human ATP6V1C1 (528) siRNA – SMARTpool and ON-TARGETplus Human ATP6V1A (523) siRNA – SMARTpool) and non-targeting siRNA (ON-TARGETplus Non-targeting Pool) were diluted with 1x siRNA buffer (Dharmacon). Cells were reverse-transfected using Dharmafect reagent (Dharmacon) following manufacturer's instructions. Cells were incubated in siRNA containing media for either 48 or 72 hours prior to

harvesting.

CRISPR editing

A stable ATP6V1C1 (ATP6V1C1-202; ENST00000518738.2) knockout was generated using the protocol of *Zhang et al.* (29). Briefly, the sgRNA sequence: GGACTGCTTGATTGGATATT **TGG** was ligated into the plasmid pSpCas9(BB)-2A-Puro (PX459) V2.0 (Addgene plasmid #62988 ; http://n2t.net/addgene:62988 ; RRID:Addgene_62988). Respective oligonucleotide sequences (Sigma) were: 5' **CACC** GGGACTGCTTGATTGGATATT 3', and 5' **AAAC** AATATCCAATCAAGCAGTCCC 3'. Cells were transfected with the sgRNA expressing plasmid using Fugene HD (Promega) with puromycin (Sigma) selection (1.5 µg/ml) for 48-72 hours. A single cell clone was isolated and validated using western blotting and Sanger sequencing.

Statistical analysis

Where indicated either two-way ANOVA with Tukey's multiple comparison post-hoc test or two-tailed Student's t-tests were used to generate P values and determine statistical significance of the indicated differences. P-values under 0.05 were considered statistically significant. Values were plotted using GraphPad Prism 7 and displayed as mean values ± standard deviation. Biological triplicates were used unless otherwise stated.

Results

V-ATPase inhibition attenuates wild-type AR signaling in HSPC cells

Androgen sensitivity and dependence is a characteristic of HSPC. We first determined the non-cytotoxic concentrations of the V-ATPase inhibitors bafilomycin-A1 (baf-A1) (30) and concanamycin-A (con-A) (31) in the HSPC LNCaP cell line (Figure 1A), as well as in HEK-293 (Figure 1B) and the androgen insensitive 22Rv1 cell line (Figure 1C). We then measured the effect of V-ATPase inhibition on wild-type AR transactivation, using the HEK-293 cell line which does not express the AR. HEK-293 cells were transfected with an androgen response element (ARE^3) reporter plasmid, a wild type-AR (AR-WT) expression plasmid and a *Renilla* transfection control plasmid. Following 24-hour exposure to 1 nM DHT, and a range of concentrations of the V-ATPase inhibitors baf-A1or con-A , levels of ARE gene activation were detected via luminescent quantification.

Consistent with previous research (26), nanomolar concentrations of baf-A1 and con-A significantly reduced AR-WT activity (Figure 2A).. We then tested the impact of V-ATPase inhibitors in the LNCaP HSPC cell line model. V-ATPase inhibition using con-A (Figure S1) or baf-A1 (Figure 2B, Figure S2) reduced expression of downstream AR targets *KLK3* (PSA*)* and *TMPRSS2* at the transcript level.

At the protein level, V-ATPase inhibition also reduced AR expression (Figure 2C) consistent with prior data in LNCaP and LAPC4 HSPC cells (23). Of note, despite reduced AR protein expression being a consistent finding, we found that V-ATPase inhibition had variable effects on PSA protein expression. In some experimental conditions we observed PSA protein increase, despite consistent PSA depletion at the transcript level (for example Figure S3).

To further investigate the potential link between V-ATPase and AR signaling we used the AR antagonist enzalutamide (which binds the AR ligand binding

domain) in LNCaP cells. When V-ATPase inhibition was combined with AR antagonism there was a significant reduction of both AR downstream transcript expression (Figure 2D) and AR protein expression (Figure 2E).

V-ATPase inhibition attenuates AR point mutant signaling

To address the impact of V-ATPase function on altered AR forms, we first utilized an AR-F877L model system for CRPC. Following validation of relative enzalutamide resistance and AR-F877L protein expression (Figure S4 and S5), we found that at nanomolar concentrations, V-ATPase chemical inhibition reduced AR-F877L transactivation activity in a same manner to AR-WT (Figure 3A).

We also investigated LNCaP cells containing the AR-F877L/T878A double mutant treated with both enzalutamide and baf-A1. In these cells AR signaling was significantly reduced compared to controls at both the mRNA (Figure 3B) and protein (Figure 3C) level, indicating V-ATPase inhibition could overcome enzalutamide resistance in an endogenous AR system. To validate these results, the experiments were repeated using a partner expression plasmid LNCaP cell line containing only the endogenous T878A mutation (Figure S6). Results using this control cell line aligned as expected with what we had previously observed in non-modified LNCaP cells (as shown in Figure 2E), confirming that F877L was driving the enzalutamide resistance.

V-ATPase inhibition reduces AR signaling in AR splice variant cell lines

Using the HEK-293 reporter assay system, V-ATPase chemical inhibition led to significant reduction in AR-V7 mediated ARE activation (Figure 4A) despite substantially higher baseline activation than for AR-WT. Similar results were obtained (Figure 4B) with a plasmid expressing AR-Q641X (p.(Gln641Xaa)) which contains a nonsense mutation in the hinge region of the AR, resulting in a constitutively active protein (32). We also found that AR expression was reduced with V-ATPase inhibition in the AR-V7-expressing 22Rv1 cell line at both the

mRNA (Figure 4C) and protein level (Figure 4D).

Genetic manipulation of the V-ATPase subunit isoform V_1C1 provides an insight into V-ATPase mediated regulation of AR expression in CRPC cells

Many V-ATPase subunits have tissue specific isoforms, with some functioning independently of the complete complex to regulate various signaling pathways (33). Various subunit isoforms are overexpressed in different cancer types compared to healthy tissue (16). This led us to question whether targeting one of these isoforms could lead to reduced V-ATPase activity, and consequently a depletion of AR activity.

The regulatory V_1C1 subunit, encoded by *ATP6V1C1*, was selected for further investigation as its overexpression in different cancer types has been linked to functional defects (34,35). Structurally, the V_1C subunit connects the V_1 and V_O domains, with detachment otherwise. In yeast, this detachment results in a loss of V-ATPase activity in a regulatory process known as reversible dissociation (36). Additionally, the V_1C1 isoform was selected over V_1C2; because V_1C1 is ubiquitously expressed, whereas V_1C2 is tissue specific (37). Interestingly, data from The Human Protein Atlas indicates that the protein levels of the V_1C1 isoform is low in prostate tissue, whereas the V_1C2 isoform is expressed at high levels (38).

Firstly, we depleted V_1C1 by siRNA knockdown to determine the effect on AR protein in 22Rv1 cells. As earlier experiments (described in Figure 4) demonstrated that AR splice variant activity is correlated to expression, only endogenous AR protein expression was investigated. To assess the specificity of effects of V_1C1 knockdown, the V_1A subunit was also depleted. The V_1A subunit has no other isoforms, and thus is an essential catalytic component of the V-ATPase complex (18). Therefore, V_1A depletion should reduce overall V-ATPase complex expression and activity. In addition to this, the expression of the alternative isoform V_1C2 was also measured in response to V_1C1 knockdown.

After 48 hours of ATP6V1C1 siRNA transfection, AR-WT protein levels were reduced (Figure 5A). Moreover, after 72 hours, AR-WT and AR-V7 levels were substantially reduced compared to the non-specific siRNA transfected controls. Additionally, AR-WT depletion was accompanied by a significant increase of V_1C2 expression, suggesting a possible compensatory role.

To investigate this further, CRISPR-Cas9 was used to eliminate V_1C1 expression. A single 22Rv1 CRISPR-Cas9 V_1C1 knockout clone (V_1C1 k/o) was validated by Sanger sequencing.In the V_1C1 depleted cells, AR-WT and AR-V7 expression was comparable to plasmid only control cells (Figure 5B). Additionally, V_1C2 protein levels were increased in the knockout cells compared to plasmid only control cells.

Discussion

Treatment options for HSPC, based on AR inhibition, are usually initially highly effective. However once the cancer becomes castrate resistant, with AR activity independent of systemic androgenic stimulation, treatment options are limited (39), with cross-resistance against AR directed drugs (40). We therefore investigated whether V-ATPase inhibition would impact AR signaling in PC driven through altered AR expression. Previous data had established a link between V-ATPase and AR signaling in HSPC (23). Here, we show that the effects of V-ATPase inhibition extend beyond HSPC models, and that V-ATPase inhibition can alter aberrant AR signaling in the form of AR splice variants and mutant AR forms.

AR splice variants, such as AR-V7 and AR-Q641X, are associated with progression to CRPC through constitutively active AR function. Moreover, functional AR activating mutations such as F877L and T878A may result in a broadening of the ligand-binding domain and resistance to clinically relevant antiandrogens including enzalutamide. We have shown that V-ATPase inhibition reduced AR-V7, AR-Q641X and AR-F877L transactivation. Additionally, V-ATPase inhibition resulted in a reduction in AR protein expression in 22Rv1 cells and LNCaP cells expressing the inducible F877L/T878A double mutant. Together, these data strengthen evidence of a link between V-ATPase and AR signaling. Most importantly, it shows that V-ATPase inhibition results in a reduction of AR signaling, which is independent of AR aberration expression. Therefore, the potential exists for V-ATPase to be developed as a therapeutic target for CRPC.

Mechanism of effect of V-ATPase inhibition on AR

The mechanism for reduced AR function resulting from V-ATPase inhibition is complex. It had been shown that inhibiting V-ATPase in prostate cancer cell lines resulted in reduced mRNA levels of downstream AR target genes such as *KLK3* (the gene for PSA). Paradoxically this was accompanied by an increase in PSA

protein levels (26). Our data validate this in both the hormone sensitive LNCaP and DuCaP cell lines. A primary function of V-ATPase is to acidify intracellular vesicles to enable functions such as receptor endocytosis and vesicular transport (41). The increase in PSA protein may potentially be explained therefore by inhibition of these key processes although the possibility of other mechanisms is acepted. Moreover, as PSA is secreted and TMPRSS2 is not, it is probable that this effect is linked to protein secretion, which occurs via the ER/Golgi pathway. It was previously suggested that V-ATPase inhibition would disrupt this secretory pathway and causes alkalinisation of transport vesicles leading to an accumulation of intracellular PSA. This accumulation of PSA might then mask downregulation of PSA mRNA resulting from potentially therapeutic V-ATPase inhibition (26). This might imply that PSA level would not be reliable as a means of therapeutic monitoring for V-ATPase inhibition in prostate cancer.

It has also been suggested that the direct effect of V-ATPase inhibition on AR levels involves HIF-1α. The proposed mechanism suggests V-ATPase inhibition results in defective transferrin receptor recycling due to alkalization of endo-lysosomal compartments. This in turn blocks iron uptake and reduces HIF-1α hydroxylation, resulting in an increase in HIF-1α stability. HIF-1α is then free to translocate to the nucleus and downregulate AR expression (23). It is also of note that knockdown of specific V-ATPase subunits (Ac45, V_Oa1 and V_Oa3) reduced transferrin receptor recycling to the plasma membrane (22). Hence targeting these subunits might reduce AR activity via a decrease in intracellular iron concentration and a reduction in HIF-1α hydroxylation. However, it was also found that co-incubation of con-A with iron significantly reduced HIF-1α protein levels, thus conflicting the suggested mechanism (23). Therefore, it is likely that the interactions between V-ATPase and the AR are multifaceted, involving several signaling pathways, and further research is required to conclusively determine the mechanism behind such interactions.

The effect of ATP6V1C1 genetic manipulation on AR expression in CRPC cells

Transient versus sustained loss of the V_1C1 subunit had substantially different effects on AR expression in 22Rv1 CRPC cells. A transient reduction (using siRNA) resulted in reduced AR expression, whereas permanent loss of V_1C1 (using CRISPR) resulted in no substantial changes in AR expression. One possible explanation, is that V_1C2 compensates for permanent loss of V_1C1 and can maintain AR signaling in 22Rv1 cells. In support of this, it was recently found that *ATP6V1C1* and *ATP6V1C2*, which encode the two V_1C isoforms, are differentially expressed in tumors from esophageal squamous cell carcinoma (ESCC) patients (42). The expression levels of the isoforms were comparable in normal esophageal tissues but in ESCC tumors *ATP6V1C1* was overexpressed and displayed tissue dominance over *ATP6V1C2* (42). Therefore, despite being described as having low protein expression in normal prostate tissue (38), it is possible that the V_1C1 subunit is overexpressed in PC cells and loss of this isoform leads to a compensatory upregulation of the V_1C2 isoform to maintain V-ATPase function. As with chemical intervention, the compensatory increase in V_1C2 expression may result in an increase in cell survival, which is of potential concern and is an important consideration for the future development of this strategy.

In addition to this, prior data exist to support the concept of V-ATPase subunit isoform compensation for another. *Kawamura et al.* generated a Cre-lox genetically modified mouse model lacking the neuronal specific V_1G2 isoform with no obvious detriment to brain architecture or phenotype (43). In this model, the V_1G1 ubiquitously expressed isoform was found to accumulate to larger amounts than in a wild-type mouse model. Interestingly, despite an increase in V_1G1 protein, there was no increase in V_1G1 mRNA, indicating that a loss of function of V_1G1 was compensated by V_1G2 without mRNA upregulation (43). In addition, another group demonstrated that the ubiquitously expressed V_1B2 isoform can compensate for the loss of the kidney specific V_1B1 isoform in medullary A intercalated cells. Apical V_1B2 immunostaining was two-fold higher in a V_1B1 null mouse model compared to one positively expressing V_1B1. The compensated V_1B2 complexes were also able to maintain 28-40% of normal V-ATPase activity, which was sufficient to maintain acid-base homeostasis in

V_1B1 deficient mice (44). Another study investigating the role of V_Oa3 in phagosome acidification found that mice deficient in V_Oa3 still exhibit V-ATPase dependent acidification, albeit to a lesser degree than in wild-type mice (45), indicating that V_Oa1 and V_Oa2 isoforms could at least partially rescue V-ATPase function.

Alternatively, as V_1C1 is involved in V-ATPase regulation (41), it is plausible that a transient reduction of the V_1C1 subunit causes aberrant V-ATPase regulation, consequently impacting upon other signaling pathways such as mTORC1. This transcriptional crosstalk with AR remains poorly understood but might represent another way the V-ATPase is linked to AR signaling. Although not investigated in this paper, due to the interactions between V-ATPase and mTORC1, it also cannot be ruled out that the V-ATPase complex, or at least its components, contribute directly to AR signaling. For example, *McConnell et al.* proposed that reducing V_1C1 expression may reduce V-ATPase assembly and prevent mTORC1 mediated cancer cell growth due to a failure of mTORC1 to receive amino acid signals (35).

Potential clinical significance

Due to ubiquitous expression, targeting the V-ATPase complex as a whole would likely be toxic with off target effects. However, this data supports that targeting specific subunit isoforms might be an efficient method of reducing AR signaling. For example, subunits such as Ac45 and the V_Oa isoforms may represent optimal targets to prevent V-ATPase mediated trafficking to downstream effector proteins (22), whereas perhaps transiently reducing the V_1C1 subunit would reduce AR signaling via alternative pathways such as mTORC1 (35). Further research is required to ascertain which subunit isoforms are of consequence in CRPC.

In this study, we have shown that combining AR inhibition (with enzalutamide) with chemical inhibition of V-ATPase has an additive effect on reducing AR functional activity. Combinatorial therapy might represent an approach to

overcome acquired resistance observed in CRPC to existing AR-directed treatments. A key area for future development would be in V-ATPase inhibitor candidates with drug-like properties.

To summarize, V-ATPase inhibition can reduce AR signaling in prostate cancer cells. Of significance we have demonstrated, for the first time, that this extends to both point mutant and splice variant AR forms that are clinically relevant for transition to CRPC. This suggests that V-ATPase could be targeted as a way to overcome AR signaling in patients with AR aberrations, including the significant unmet clinical need that exists for patients with CRPC.

Acknowledgments: BW was funded by a doctoral studentship from The Urology Foundation, Wessex Medical Research and The Gerald Kerkut Charitable Trust. This work was also supported by grants from Cancer Research UK (C2750/A23669).

References

1. Culp MB, Soerjomataram I, Efstathiou JA, Bray F, Jemal A. Recent Global Patterns in Prostate Cancer Incidence and Mortality Rates. Eur Urol **2020**;77(1):38-52.
2. James ND, Spears MR, Clarke NW, Dearnaley DP, De Bono JS, Gale J*, et al.* Survival with Newly Diagnosed Metastatic Prostate Cancer in the "Docetaxel Era": Data from 917 Patients in the Control Arm of the STAMPEDE Trial (MRC PR08, CRUK/06/019). Eur Urol **2015**;67(6):1028-38.
3. Jernberg E, Bergh A, Wikström P. Clinical relevance of androgen receptor alterations in prostate cancer. **2017**;6(8):R146.
4. Joseph JD, Lu N, Qian J, Sensintaffar J, Shao G, Brigham D*, et al.* A clinically relevant androgen receptor mutation confers resistance to second-generation antiandrogens enzalutamide and ARN-509. Cancer Discov **2013**;3(9):1020-9.
5. Korpal M, Korn JM, Gao X, Rakiec DP, Ruddy DA, Doshi S*, et al.* An F876L Mutation in Androgen Receptor Confers Genetic and Phenotypic Resistance to MDV3100 (Enzalutamide). Cancer Discov **2013**;3(9):1030-43.
6. Fenton MA, Shuster TD, Fertig AM, Taplin ME, Kolvenbag G, Bubley GJ*, et al.* Functional characterization of mutant androgen receptors from androgen-independent prostate cancer. Clin Cancer Res **1997**;3(8):1383-8.
7. Taplin M-E, Bubley GJ, Ko Y-J, Small EJ, Upton M, Rajeshkumar B*, et al.* Selection for Androgen Receptor Mutations in Prostate Cancers Treated with Androgen Antagonist. Cancer Res **1999**;59(11):2511-5.
8. Culig Z, Hobisch A, Cronauer MV, Cato AC, Hittmair A, Radmayr C*, et al.* Mutant androgen receptor detected in an advanced-stage prostatic carcinoma is activated by adrenal androgens and progesterone. Mol Endocrinol **1993**;7(12):1541-50.
9. Chen EJ, Sowalsky AG, Gao S, Cai C, Voznesensky O, Schaefer R*, et al.* Abiraterone treatment in castration-resistant prostate cancer selects for

progesterone responsive mutant androgen receptors. Clin Cancer Res **2015**;21(6):1273-80.

10. Sun S, Sprenger CCT, Vessella RL, Haugk K, Soriano K, Mostaghel EA*, et al.* Castration resistance in human prostate cancer is conferred by a frequently occurring androgen receptor splice variant. J Clin Invest **2010**;120(8):2715-30.
11. Antonarakis ES, Lu C, Wang H, Luber B, Nakazawa M, Roeser JC*, et al.* AR-V7 and Resistance to Enzalutamide and Abiraterone in Prostate Cancer. NEJM **2014**;371(11):1028-38.
12. Sharp A, Coleman I, Yuan W, Sprenger C, Dolling D, Rodrigues DN*, et al.* Androgen receptor splice variant-7 expression emerges with castration resistance in prostate cancer. J Clin Invest **2019**;129(1):192-208.
13. Welti J, Sharp A, Yuan W, Dolling D, Nava Rodrigues D, Figueiredo I*, et al.* Targeting Bromodomain and Extra-Terminal (BET) Family Proteins in Castration-Resistant Prostate Cancer (CRPC). Clin Cancer Res **2018**;24(13):3149-62.
14. Hu R, Dunn TA, Wei S, Isharwal S, Veltri RW, Humphreys E*, et al.* Ligand-independent Androgen Receptor Variants Derived from Splicing of Cryptic Exons Signify Hormone Refractory Prostate Cancer. Cancer Res **2009**;69(1):16-22.
15. Qu Y, Dai B, Ye D, Kong Y, Chang K, Jia Z*, et al.* Constitutively active AR-V7 plays an essential role in the development and progression of castration-resistant prostate cancer. Sci Rep **2015**;5:7654-.
16. Whitton B, Okamoto H, Packham G, Crabb SJ. Vacuolar ATPase as a potential therapeutic target and mediator of treatment resistance in cancer. Cancer Med **2018**;7(8):3800-11.
17. Marshansky V, Futai M. The V-type H+-ATPase in vesicular trafficking: targeting, regulation and function. Curr Opin Cell Biol **2008**;20(4):415-26.
18. Toei M, Saum R, Forgac M. Regulation and Isoform Function of the V-ATPases. Biochemistry **2010**;49(23):4715-23.
19. Marshansky V. The V-ATPase a2-subunit as a putative endosomal pH-sensor. Biochem Soc Trans **2007**;35(Pt 5):1092-9.
20. Zoncu R, Bar-Peled L, Efeyan A, Wang S, Sancak Y, Sabatini DM.

mTORC1 senses lysosomal amino acids through an inside-out mechanism that requires the vacuolar H(+)-ATPase. Science **2011**;334(6056):678-83.

21. Licon-Munoz Y, Michel V, Fordyce CA, Parra KJ. F-actin reorganization by V-ATPase inhibition in prostate cancer. Biol Open **2017**;6(11):1734-44.
22. Smith GA, Howell GJ, Phillips C, Muench SP, Ponnambalam S, Harrison MA. Extracellular and Luminal pH Regulation by Vacuolar H+-ATPase Isoform Expression and Targeting to the Plasma Membrane and Endosomes. J Biol Chem **2016**;291(16):8500-15.
23. Licon-Munoz Y, Fordyce CA, Hayek SR, Parra KJ. V-ATPase-dependent repression of androgen receptor in prostate cancer cells. Oncotarget **2018**;9(48):28921-34.
24. Fan S, Niu Y, Tan N, Wu Z, Wang Y, You H*, et al.* LASS2 enhances chemosensitivity of breast cancer by counteracting acidic tumor microenvironment through inhibiting activity of V-ATPase proton pump. Oncogene **2013**;32(13):1682-90.
25. Sennoune SR, Bermudez LE, Lees JC, Hirsch J, Filleur S, Martinez-Zaguilan R. Vacuolar H+-ATPase is down-regulated by the angiogenesis-inhibitory pigment epithelium-derived factor in metastatic prostate cancer cells. Cell Mol Biol (Noisy-le-grand) **2014**;60(1):45-52.
26. Michel V, Licon-Munoz Y, Trujillo K, Bisoffi M, Parra KJ. Inhibitors of vacuolar ATPase proton pumps inhibit human prostate cancer cell invasion and prostate-specific antigen expression and secretion. Int J Cancer **2013**;132(2):E1-10.
27. Regufe da Mota S, Bailey S, Strivens RA, Hayden AL, Douglas LR, Duriez PJ*, et al.* LSD1 inhibition attenuates androgen receptor V7 splice variant activation in castration resistant prostate cancer models. Cancer Cell Int **2018**;18:71-.
28. Cottard F, Asmane I, Erdmann E, Bergerat JP, Kurtz JE, Ceraline J. Constitutively active androgen receptor variants upregulate expression of mesenchymal markers in prostate cancer cells. PLoS One **2013**;8(5):e63466.
29. Ran FA, Hsu PD, Wright J, Agarwala V, Scott DA, Zhang F. Genome

engineering using the CRISPR-Cas9 system. Nat Protoc **2013**;8:2281.

30. Werner G, Hagenmaier H, Drautz H, Baumgartner A, Zähner H. Metabolic products of microorganisms. 224. Bafilomycins, a new group of macrolide antibiotics. Production, isolation, chemical structure and biological activity. The Journal of antibiotics **1984**;37(2):110-7.
31. Westley JW, Liu CM, Sello LH, Evans RH, Troupe N, Blount JF*, et al.* The structure and absolute configuration of the 18-membered macrolide lactone antibiotic X-4357B (concanamycin A). The Journal of antibiotics **1984**;37(12):1738-40.
32. Ceraline J, Cruchant MD, Erdmann E, Erbs P, Kurtz JE, Duclos B*, et al.* Constitutive activation of the androgen receptor by a point mutation in the hinge region: a new mechanism for androgen-independent growth in prostate cancer. Int J Cancer **2004**;108(1):152-7.
33. Maxson ME, Grinstein S. The vacuolar-type H⁺-ATPase at a glance – more than a proton pump. J Cell Sci **2014**;127(23):4987-93.
34. Garcia-Garcia A, Perez-Sayans Garcia M, Rodriguez MJ, Antunez-Lopez J, Barros-Angueira F, Somoza-Martin M*, et al.* Immunohistochemical localization of C1 subunit of V-ATPase (ATPase C1) in oral squamous cell cancer and normal oral mucosa. Biotech Histochem **2012**;87(2):133-9.
35. McConnell M, Feng S, Chen W, Zhu G, Shen D, Ponnazhagan S*, et al.* Osteoclast proton pump regulator Atp6v1c1 enhances breast cancer growth by activating the mTORC1 pathway and bone metastasis by increasing V-ATPase activity. Oncotarget **2017**;8(29):47675-90.
36. Oot RA, Huang L-S, Berry EA, Wilkens S. Crystal structure of the yeast vacuolar ATPase heterotrimeric EGC(head) peripheral stalk complex. Structure (London, England : 1993) **2012**;20(11):1881-92.
37. Sun-Wada GH, Murata Y, Namba M, Yamamoto A, Wada Y, Futai M. Mouse proton pump ATPase C subunit isoforms (C2-a and C2-b) specifically expressed in kidney and lung. J Biol Chem **2003**;278(45):44843-51.
38. Pontén F, Jirström K, Uhlen M. The Human Protein Atlas--a tool for pathology. The Journal of pathology **2008**;216(4):387-93.
39. Nevedomskaya E, Baumgart SJ, Haendler B. Recent Advances in

Prostate Cancer Treatment and Drug Discovery. Int J Mol Sci **2018**;19(5):1359.

40. Nakazawa M, Paller C, Kyprianou N. Mechanisms of Therapeutic Resistance in Prostate Cancer. Curr Oncol Rep **2017**;19(2):13-.
41. Cotter K, Stransky L, McGuire C, Forgac M. Recent Insights into the Structure, Regulation, and Function of the V-ATPases. Trends Biochem Sci **2015**;40(10):611-22.
42. Couto-Vieira J, Nicolau-Neto P, Costa EP, Figueira FF, Simão TdA, Okorokova-Façanha AL*, et al.* Multi-cancer V-ATPase molecular signatures: A distinctive balance of subunit C isoforms in esophageal carcinoma. EBioMedicine **2020**;51.
43. Kawamura N, Sun-Wada G-H, Wada Y. Loss of G2 subunit of vacuolar-type proton transporting ATPase leads to G1 subunit upregulation in the brain. Sci Rep **2015**;5:14027.
44. Păunescu TG, Rodriguez S, Benz E, McKee M, Tyszkowski R, Albers MW*, et al.* Loss of the V-ATPase B1 Subunit Isoform Expressed in Non-Neuronal Cells of the Mouse Olfactory Epithelium Impairs Olfactory Function. PLoS One **2012**;7(9):e45395.
45. Sun-Wada GH, Tabata H, Kawamura N, Aoyama M, Wada Y. Direct recruitment of H+-ATPase from lysosomes for phagosomal acidification. J Cell Sci **2009**;122(Pt 14):2504-13.

Figure Legends

Figure 1. MTS assay to determine cell line toxicity in response to bafilomycin-A1 and concanamycin-A

The indicated cell lines were treated with either 100 nM, 10 nM or 1 nM bafilomycin-A1 (baf-A1) or concanamycin-A (con-A) for 24 hours, and MTS assay data is presented relative to the DMSO treated cells set to 100% viability. Values were then plotted using GraphPad Prism 7 and are displayed as mean values ± standard deviation (SD). Two-way ANOVA with Tukey's multiple comparison post-hoc test was used to generate P values and detect the statistical significance of the indicated differences: * = p≤ 0.05, ** = p≤ 0.01, *** = p≤ 0.001

Figure 2. V-ATPase inhibition attenuates wild-type AR transactivation

(A) HEK-293 cells were transfected with an androgen response element (ARE) reporter plasmid and wild-type AR expression plasmid along with a *Renilla* luciferase plasmid. Cells were cultured in CSS-RPMI media and treated with 1 nM dihydro-testosterone (DHT) and indicated concentrations of bafilomycin-A1 (baf-A1) or concanamycin-A (con-A) for 24 hours. Firefly luciferase values were normalised to DMSO control cells set to 1. (B) LNCaP cells were treated for 24 hours with 1 nM DHT, 10 nM baf-A1 or both. RT-qPCR analysis was undertaken for mRNA levels of *PSA* and *TMPRSS2* normalised to *GAPDH*, relative to DMSO treated control cells set to 1. (C) LNCaP cells were treated for 24 hours with 1 nM DHT, 10 nM baf-A1 or both. Protein expression was measured using western blotting. RPMI, control sample. (D) LNCaP cells were treated for 24 hours with 1 nM DHT, 10 nM baf-A1, 10 μM enzalutamide (enz) or an indicated combination. RT-qPCR analysis was undertaken for mRNA levels of *PSA* and *TMPRSS2* normalised to GAPDH, relative to DMSO treated control cells set to 1. Two-way ANOVA with Tukey's multiple comparison post-hoc test was used to generate P values for the indicated differences: ns = non-significant, **= p≤ 0.01, **** = p≤ 0.0001. (E) LNCaP cells were treated for 24 hours with 1 nM DHT, 10 nM baf-A1, 10 μM enz or a combination of each. Protein expression was measured using western blotting. Densitometry graphs show mean (±SD) expression with values for CSS-RPMI cells set to 1.0, and the statistical

significance of the indicated differences (Student's t-test). RPMI, control sample.

Figure 3. V-ATPase inhibition attenuates AR-F877L signaling

(A) HEK-293 cells were transfected with an androgen response element (ARE) reporter plasmid, wild-type AR or AR-F877L expression plasmids along with a *Renilla* luciferase plasmid. Cells were cultured in CSS-RPMI media and treated with 1 nM dihydro-testosterone (DHT) and indicated concentrations of bafilomycin-A1 (baf-A1) or concanamycin-A (con-A) for 24 hours. Firefly luciferase values were normalised to DMSO control cells set to 1. (B) LNCaP cells containing F877L/T878A double AR mutations were treated with 2 μM doxycycline for 72 hours. A control sample was maintained in RPMI with equivalent concentration of DMSO. Cells were treated for 24 hours with 1 nM DHT, 10 nM baf-A1, 10 μM enzalutamide (enz) or an indicated combination. RT-qPCR analysis was undertaken for mRNA levels of *PSA* and *TMPRSS2* normalised to *GAPDH*, relative to DMSO treated control cells set to 1. Two-way ANOVA with Tukey's multiple comparison post-hoc test was used to generate P values for the indicated differences: **** = p≤ 0.0001.. (C) LNCaP cells containing F877L/T878A double AR mutations were treated with 2 μM doxycycline for 72 hours. Cells were treated for 24 hours with 1 nM DHT, 10 nM baf-A1, 10 μM enz or an indicated combination. A control LNCaP sample was maintained in RPMI and protein expression measured using western blotting. Densitometry graphs show mean (±SD) expression with values for CSS-RPMI cells set to 1.0, and the statistical significance of the indicated differences (Student's t-test).

Figure 4. V-ATPase inhibition reduces AR signaling in AR splice variant cell lines

(A) HEK-293 cells were transfected with an androgen response element (ARE) reporter plasmid and wild-type AR (AR-WT) or AR-V7 expression plasmids along with a *Renilla* luciferase plasmid. Cells were cultured in CSS-RPMI media and treated with 1 nM dihydro-testosterone (DHT) and indicated concentrations of bafilomycin-A1 (baf-A1) or concanamycin-A (con-A) for 24 hours. Firefly luciferase values were normalised to DMSO control cells set to 1. (B) HEK-293

cells were transfected with the ARE reporter plasmid and wild-type AR or AR-Q641X expression plasmids along with a *Renilla* luciferase plasmid. Cells were treated with 1 nM DHT and indicated concentrations of baf-A1 or con-A for 24 hours. Firefly luciferase values were normalised to DMSO control cells set to 1. (C) 22Rv1 cells were treated for 24 hours with 1 nM DHT, 10 nM baf-A1 or both. RT-qPCR analysis for mRNA levels of *PSA* and *TMPRSS2* were normalised to *GAPDH*, relative to DMSO treated control cells set to 1. Two-way ANOVA with Tukey's multiple comparison post-hoc test was used to generate P values for the indicated differences: ns = non-significant, *** = p≤ 0.001, **** = p≤ 0.0001. (D) 22Rv1 cells were treated for 24 hours with 1 nM DHT, 10 nM baf-A1 or both. A control 22Rv1 sample was maintained in RPMI. Protein expression was measured using western blotting. Densitometry graphs show mean (±SD) expression with values for CSS-RPMI cells set to 1.0, and the statistical significance of the indicated differences (Student's t-test).

Figure 5. Genetic manipulation of the V-ATPase subunit isoform V_1C1 provides insight into V-ATPase mediated regulation of AR expression in CRPC cells

(A) 22Rv1 cells were reverse transfected with either 25 nmol of ATP6V1C1, ATP6V1A or non-specific siRNA (NS) for 48 or 72 hours. Control non-transfected cells were treated with equivalent Dharmafect 1 reagent concentrations. (B) 22Rv1 plasmid only control cells and 22Rv1-V_1C1 CRISPR knockout cells (k/o) were treated for 24 hours with 1 nM dihydro-testosterone (DHT), 10 μM enzalutamide (enz) or both. Additional LNCaP samples were also included, which were maintained in RPMI only. Protein expression was measured using western blotting. Densitometry graphs show mean (±SD) expression with values for either non-specific siRNA control or CSS-RPMI cells set to 1.0, and the statistical significance of the indicated differences (Student's t-test).

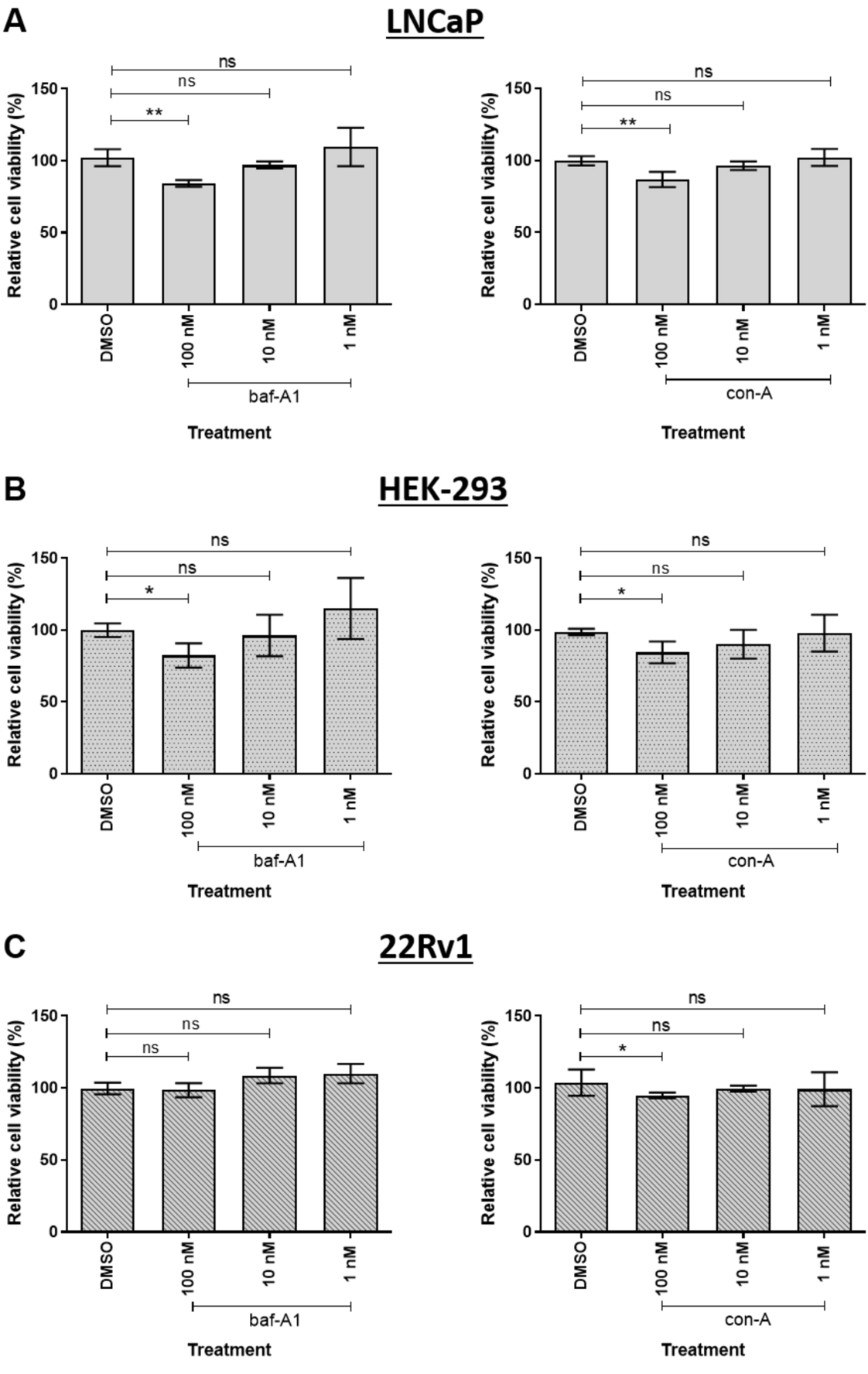
A
LNCaP
ns
ns
**
Relative cell viability (%)
150
100
50
0
DMSO
100 nM
10 nM
1 nM
baf-A1
Treatment
ns
ns
**
Relative cell viability (%)
150
100
50
0
DMSO
100 nM
10 nM
1 nM
con-A
Treatment
B
HEK-293
ns
ns
*
Relative cell viability (%)
150
100
50
0
DMSO
100 nM
10 nM
1 nM
baf-A1
Treatment
ns
ns
*
Relative cell viability (%)
150
100
50
0
DMSO
100 nM
10 nM
1 nM
con-A
Treatment
C
22Rv1
ns
ns
ns
Relative cell viability (%)
150
100
50
0
DMSO
100 nM
10 nM
1 nM
baf-A1
Treatment
ns
ns
*
Relative cell viability (%)
150
100
50
0
DMSO
100 nM
10 nM
1 nM
con-A
Treatment

Figure 1

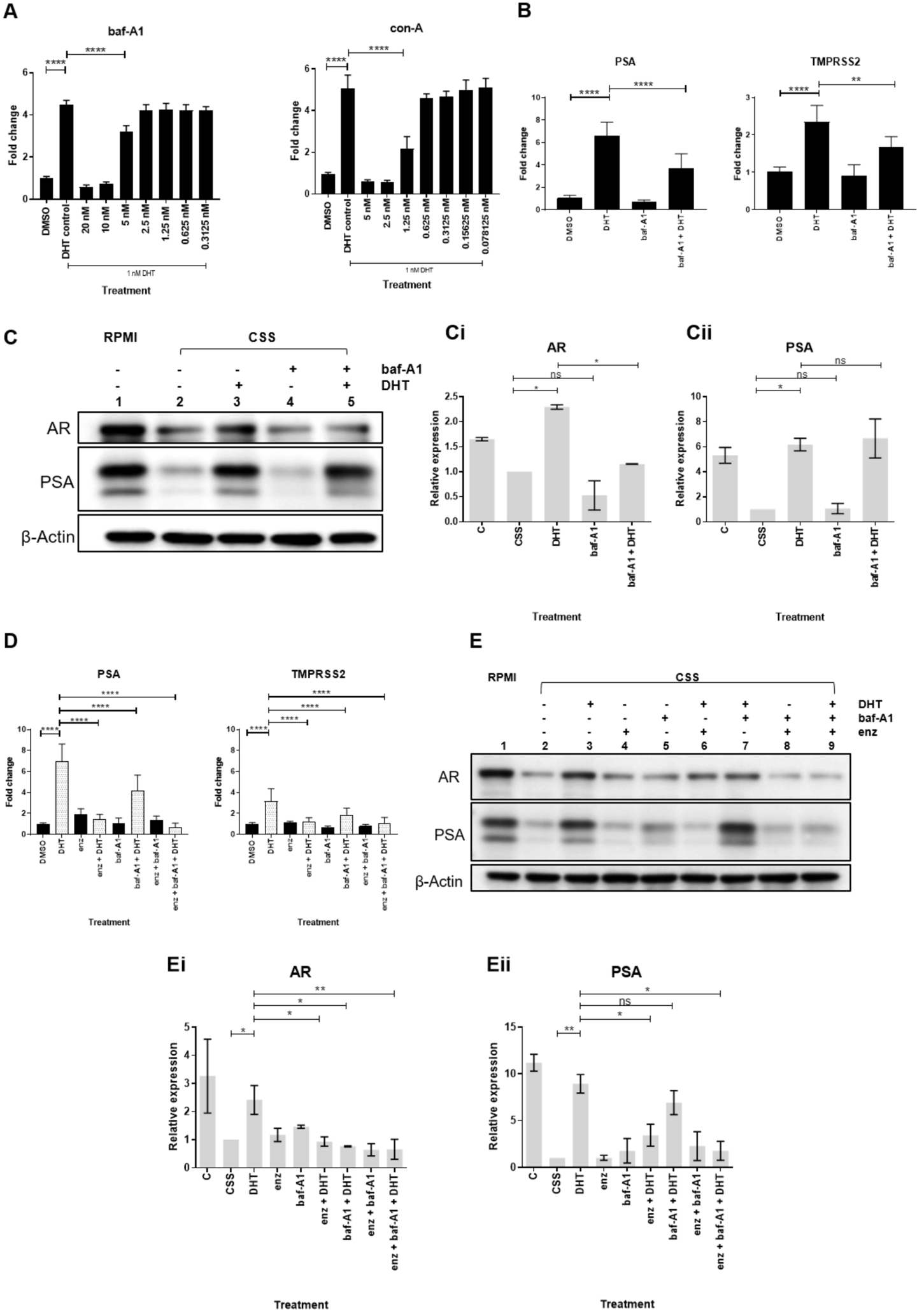
A
baf-A1
con-A
Fold change
DMSO
DHT control
20 nM
10 nM
5 nM
2.5 nM
1.25 nM
0.625 nM
0.3125 nM
5 nM
2.5 nM
1.25 nM
0.625 nM
0.3125 nM
0.15625 nM
0.078125 nM
1 nM DHT
Treatment
B
PSA
TMPRSS2
DMSO
DHT
baf-A1
baf-A1 + DHT
C
RPMI
CSS
baf-A1
DHT
AR
PSA
β-Actin
Ci
AR
Cii
PSA
Relative expression
C
CSS
DHT
baf-A1
baf-A1 + DHT
Treatment
D
PSA
TMPRSS2
enz
enz + DHT
enz + baf-A1
enz + baf-A1 + DHT
E
RPMI
CSS
DHT
baf-A1
enz
Ei
AR
Eii
PSA

Figure 2

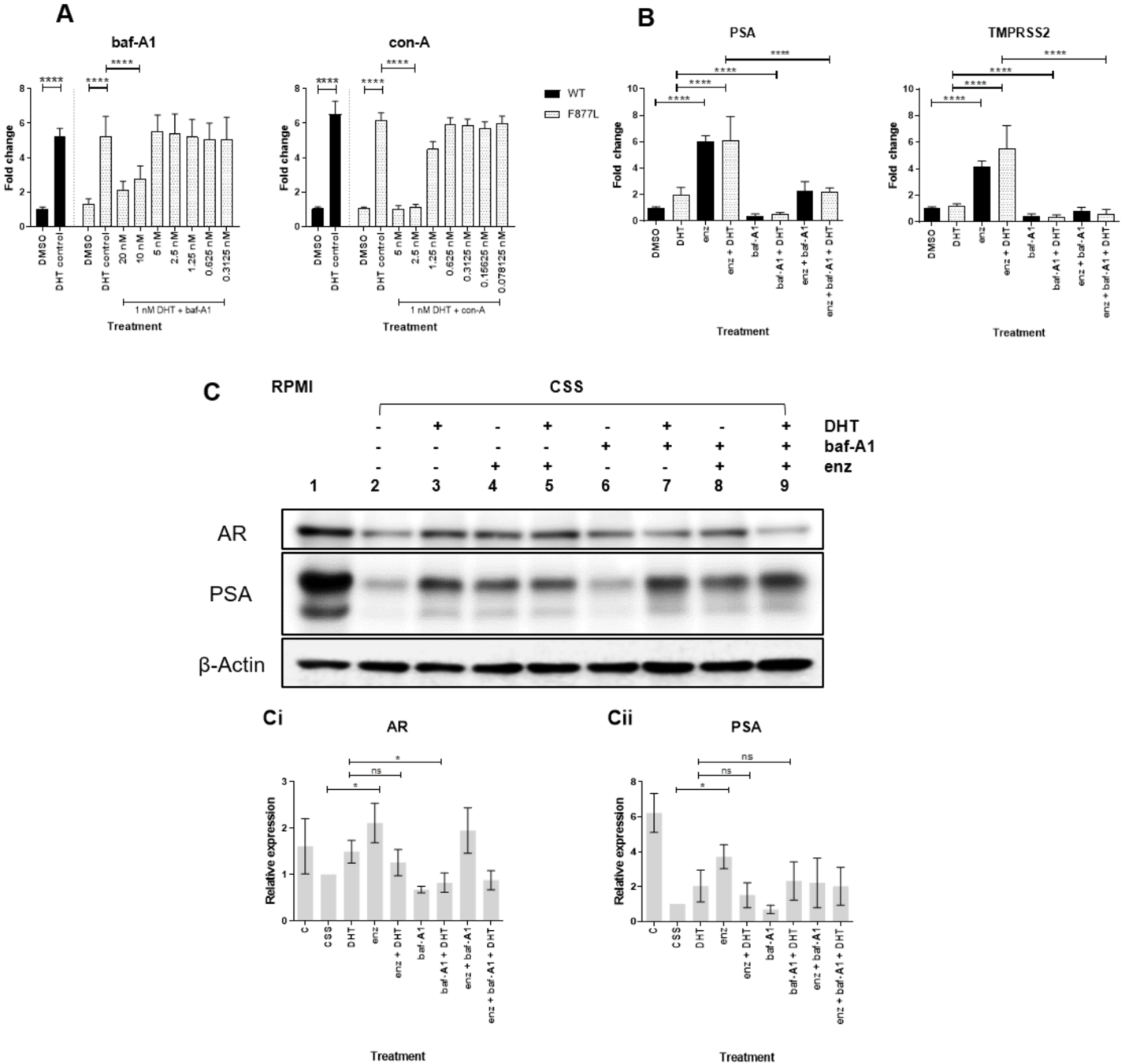
A
baf-A1
con-A
WT
F877L
Fold change
DMSO
DHT control
20 nM
10 nM
5 nM
2.5 nM
1.25 nM
0.625 nM
0.3125 nM
0.15625 nM
0.078125 nM
1 nM DHT + baf-A1
1 nM DHT + con-A
Treatment
B
PSA
TMPRSS2
DHT
enz
enz + DHT
baf-A1
baf-A1 + DHT
enz + baf-A1
enz + baf-A1 + DHT
C
RPMI
CSS
DHT
baf-A1
enz
AR
PSA
β-Actin
Ci
Cii
Relative expression
ns
C
CSS

Figure 3

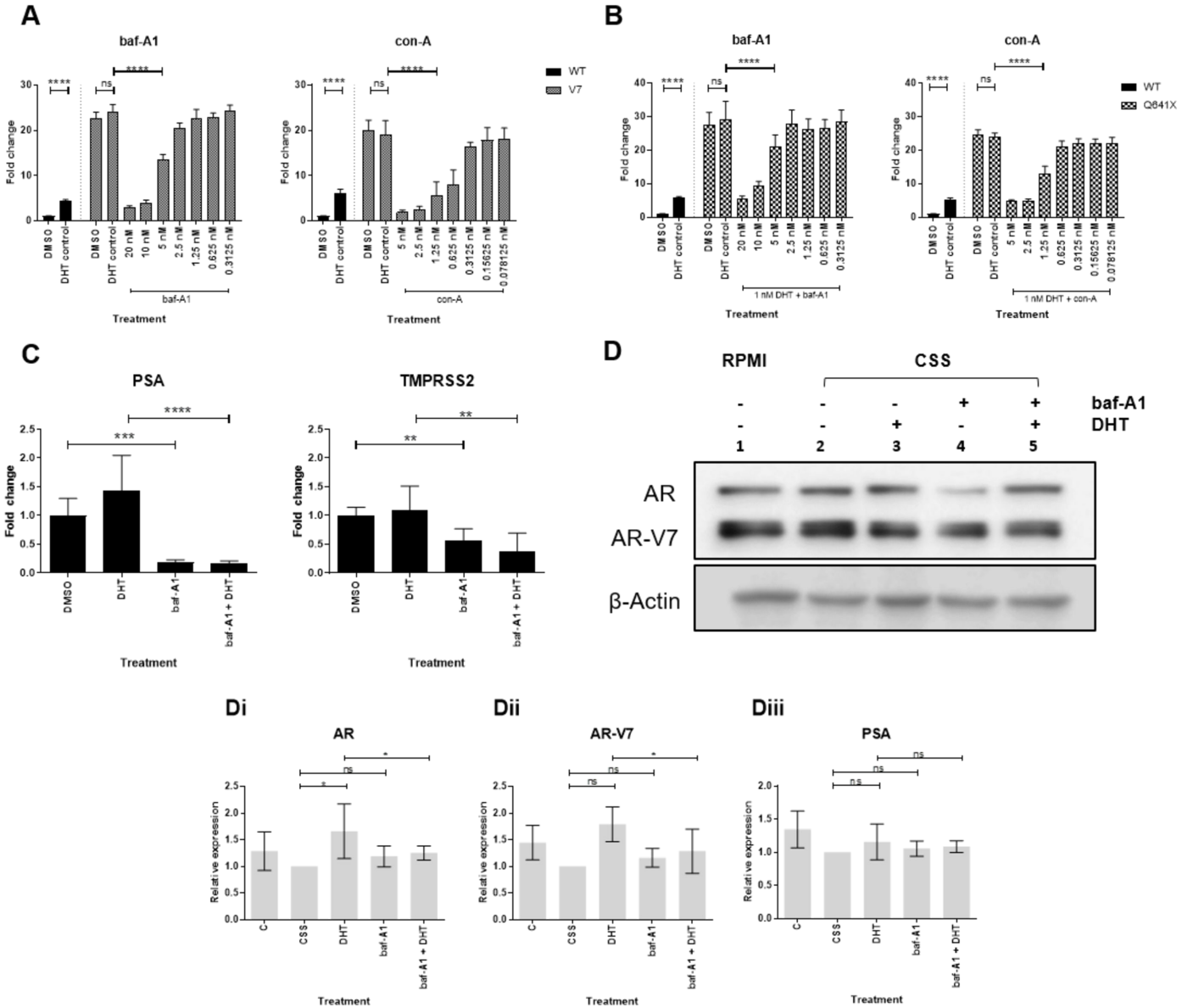
A
baf-A1
con-A
WT
V7
Fold change
Treatment
DMSO
DHT control
baf-A1
con-A
B
baf-A1
con-A
WT
Q841X
1 nM DHT + baf-A1
1 nM DHT + con-A
C
PSA
TMPRSS2
DHT
baf-A1 + DHT
D
RPMI
CSS
baf-A1
DHT
AR
AR-V7
β-Actin
Di
AR
Dii
AR-V7
Diii
PSA
Relative expression
C
CSS

Figure 4

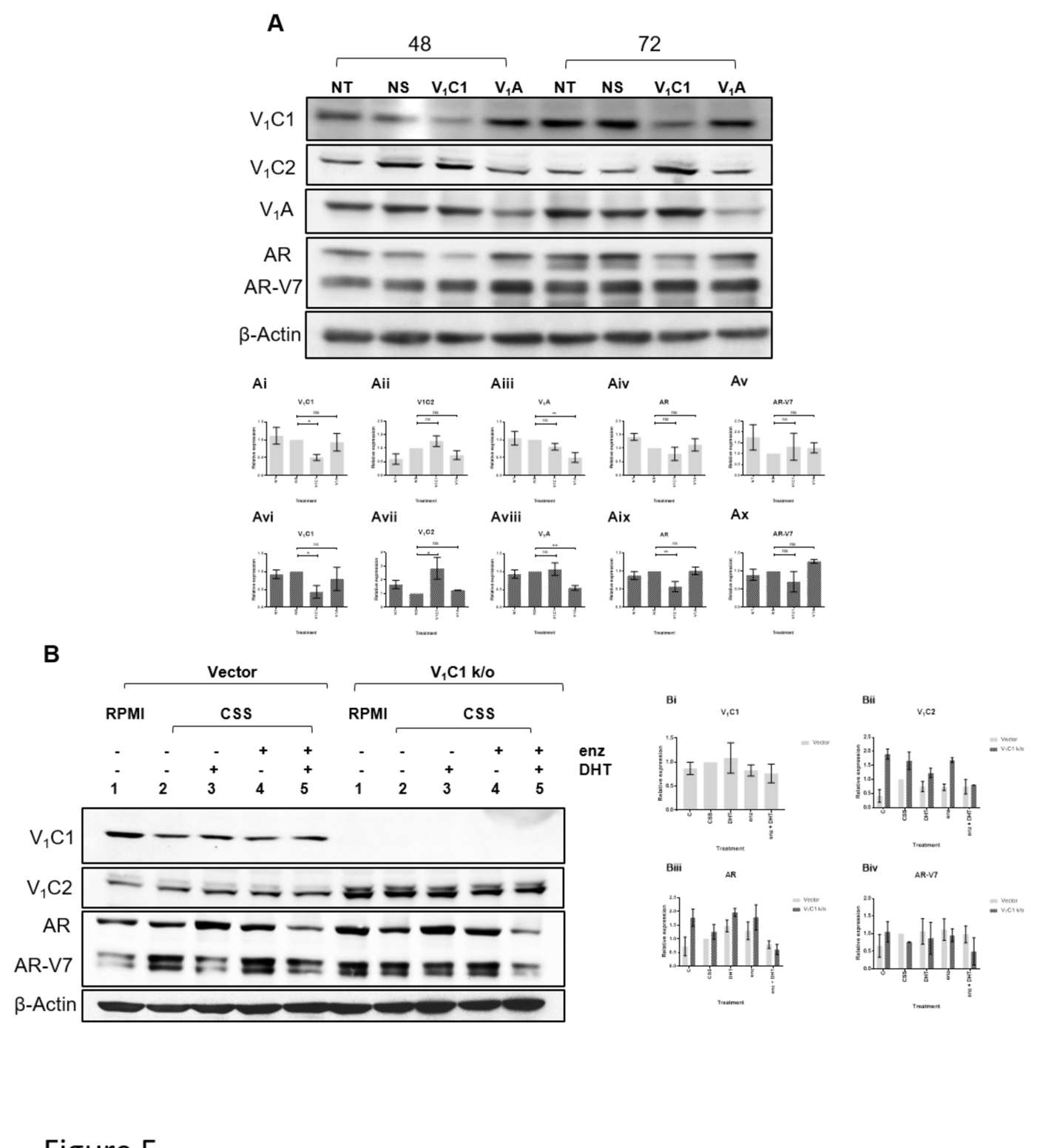
A
48
72
NT
NS
V1C1
V1A
NT
NS
V1C1
V1A
V1C1
V1C2
V1A
AR
AR-V7
β-Actin
Ai
Aii
Aiii
Aiv
Av
Avi
Avii
Aviii
Aix
Ax
B
Vector
V1C1 k/o
RPMI
CSS
RPMI
CSS
enz
DHT
1
2
3
4
5
1
2
3
4
5
V1C1
V1C2
AR
AR-V7
β-Actin
Bi
Bii
Biii
Biv
Vector
V1C1 k/o
Relative expression
Treatment

Figure 5